Supplement of Atmos. Chem. Phys., 16, 2631–2640, 2016
http://www.atmos-chem-phys.net/16/2631/2016/
doi:10.5194/acp-16-2631-2016-supplement

Atmospheric Chemistry and Physics
Open Access

Supplement of

The real part of the refractive indices and effective densities for chemically segregated ambient aerosols in Guangzhou measured by a single-particle aerosol mass spectrometer

Guohua Zhang et al.

Correspondence to: Xinhui Bi (bixh@gig.ac.cn)

1 The meteorological conditions over the study

Temporal profiles (in 1 hour resolution) of local meteorological parameters, including solar radiation, temperature (Temp), relative humidity (RH), wind direction (WD) and wind speed (WS), and air quality parameters (i.e., NO_x, SO_2, O_3, PM_1) are shown in Fig. S1. These parameters were provided by Guangdong Environmental Monitoring Center (http://www.gdemc.gov.cn/). Ambient Temp, RH, and WS over the study varied between 10.8–31 °C, 20.7–89.8%, and 0.2–3.9 m/s, with average values of 21.2 °C, 59.9%, and 1.1 m/s, respectively. The concentration peaks for NO_x, SO_2, and PM_1 were often observed during the nighttime, due to the accumulation of pollutants under unfavorable meteorological conditions with lower WS and lower boundary layer depth.

2 The mass spectral patterns for the single particle types

The mass spectral characteristics are displayed in Fig. S4, and a brief description is provided as follows.

OC group: Mass spectra for OC particles mainly contain the OC markers, and also some other OC peaks such as 50$[C_4H_2]^+$, 51$[C_4H_3]^+$, 55$[C_4H_7]^+$ and 63$[C_5H_3]^+$**.** Besides, a large peak at m/z 39 is also observed in mass spectra of OC, which might be explained by coagulation between OC and 39$[K]^+$ or condensation of organic species onto biomass seed [*Moffet et al.*, 2008]. Particle mass spectra in HMOC type show the presence of m/z 50, 51, 63, 77, 91, 115, and 128 [*Silva and Prather*, 2000; *Sodeman et* *al.*, 2005]. By including the ion peak from sulfate/nitrate, OC particles were subdivised into OC-S, OC-SN, and HMOC.

EC group: Mass spectra of LC-EC type are dominated by the distinct carbon ion clusters ranged from m/z -120 to m/z 180, with minor ion intensities from other species. SC-EC type is associated with short carbon clusters ions peaks ($C_n^{+/-}$, n < 6), generally internally mixed with intense sulfate ion peak. Differently, NaK-EC type shows the carbon ion clusters mainly in the negative mass spectra, combined with dominant peaks from 23$[Na]^+$ and 39$[K]^+$ in the positive ones.

ECOC group: ECOC particles have typical carbon ion clusters (12$[C]^{+/-}$, 24$[C_2]^{+/-}$, … , 12n$[C_n]^{+/-}$) with 36$[C_3]^+$ as dominant fragments, together with OC markers (e.g., 27$[C_2H_3]^+$, 29$[C_2H_5]^+$, 37$[C_3H]^+$, and 43$[C_2H_3O]^+$). K-rich particles contain potassium (39$[K]^+$), sulfate (-97$[HSO_4]^-$), nitrate (-46$[NO_2]^-$ and -62$[NO_3]^-$), and carbonaceous species (e.g., 12$[C]^+$, **2**7$[C_2H_3]^+$, 29$[C_2H_5]^+$, 36$[C_3]^+$, 37$[C_3H]^+$, 43$[C_2H_3O]^+$, -26$[CN]^-$, -42$[CNO]^-$) as major components, similar to those reported in other studies [*Moffet et al.*, 2008; *Silva et al.*, 1999]. The association of sulfate and/or nitrate separated the ECOC particles into ECOC-S, ECOC-SN, K-S, K-SN, and K-N [*Zhang et al.*, 2015].

Metal rich group: Peaks corresponding to **23**$[Na]^+$, 39$[K]^+$, 46$[Na_2]^+$, 81/83$[Na_2Cl]^+$, nitrate and chloride (-35$[Cl]^-$ and -37$[Cl]^-$) are present in mass spectra of Na-rich, indicating transport and evolution of sea salt particles [*Gaston et al.*, 2011; *Gaston et al.*, 2013]. Na-K type is characterized by dominant peaks from 39$[K]^+$, relatively less intense peak from **23**$[Na]^+$, nitrate and silicate (-76$[SiO_3]^-$). They are probably from dust and/or industry sources [*Moffet et al.*, 2008]. Fe-rich type is identified by strong peaks from iron at m/z 54, 56 and 57, according to their isotopic components. Similarly, Pb-rich type is identified by strong peaks m/z 206-208, and Cu-rich is characterized by the presence of isotopic peaks at m/z 63 and 65. Fe-Cu-Pb represents the internally mixed Fe, Cu, Pb in the individual particles.

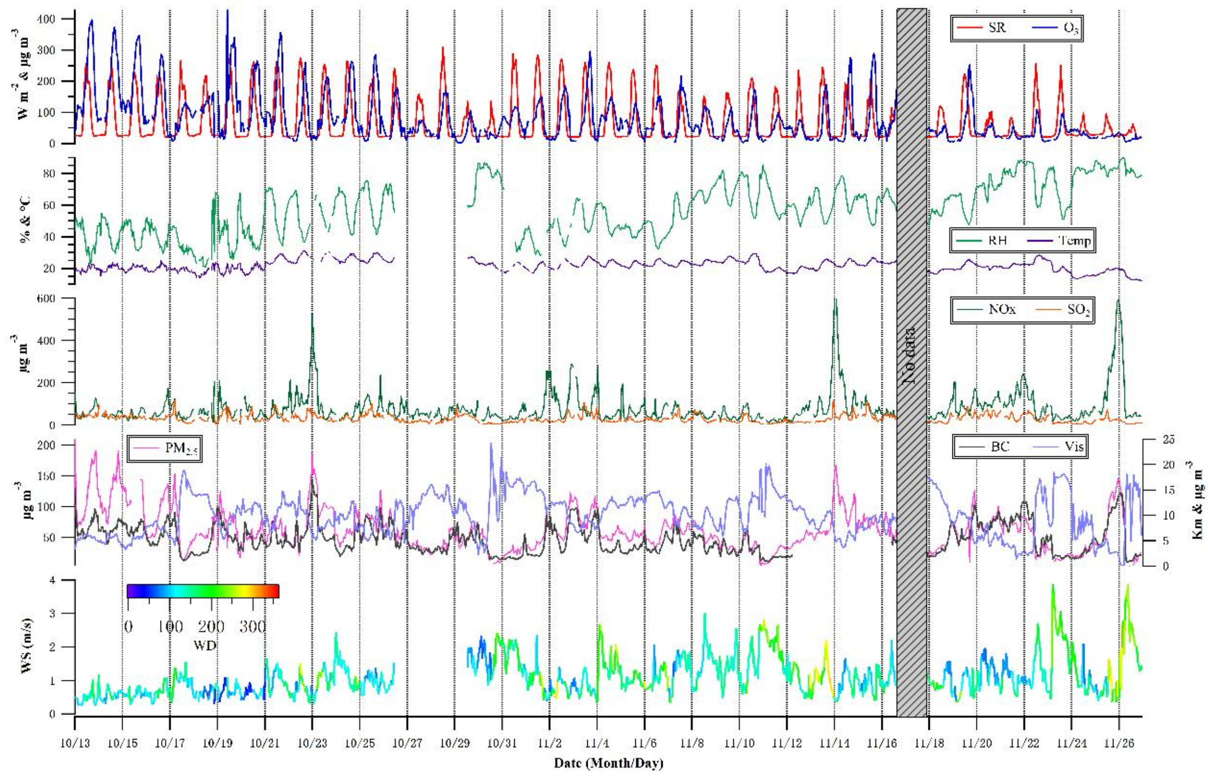

Fig. S1. Temporal profiles (in 1 h resolution) of PM_1, visibility, and black carbon (BC), gaseous pollutants (SO_2, NO_x, and O_3) and meteorological parameters, during the 13th October–26th November 2012 in Guangzhou.

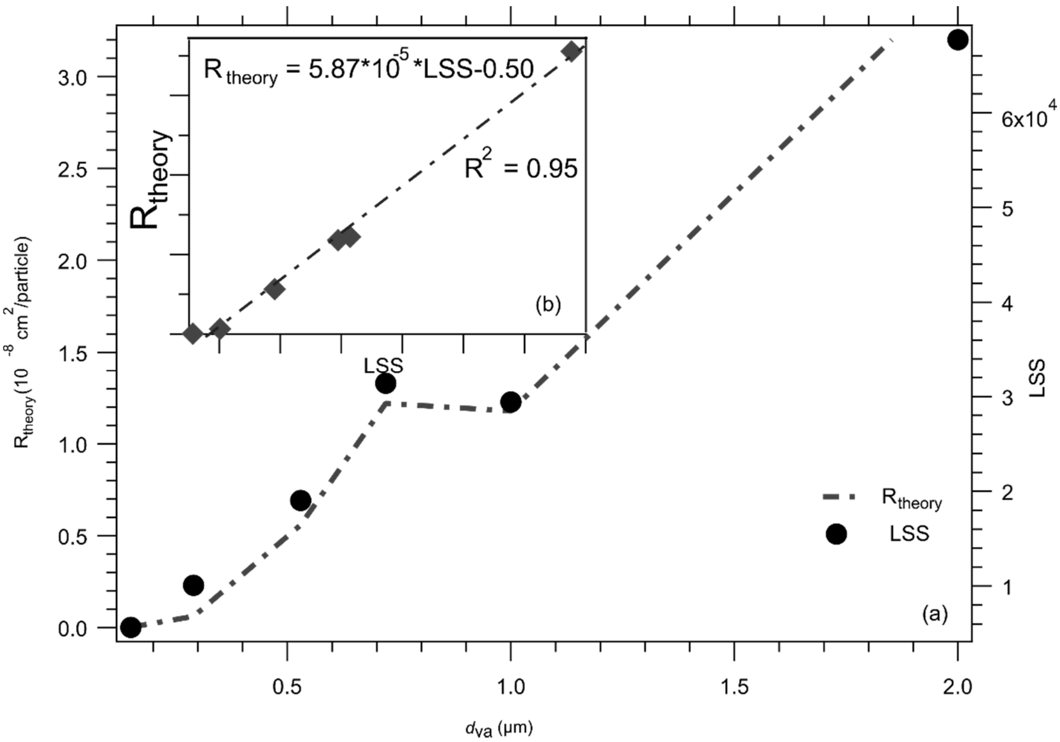

Fig. S2. (a) Upper limit of light scattering signals and theoretical PSCS for PSL as a function of size (0.15, 0.3, 0.5, 0.72, 1, and 2 μm) and (b) their relationship. For PSL, n = 1.59 and $\rho_{eff} = \rho_p = 1.054$ g cm^{-3}.

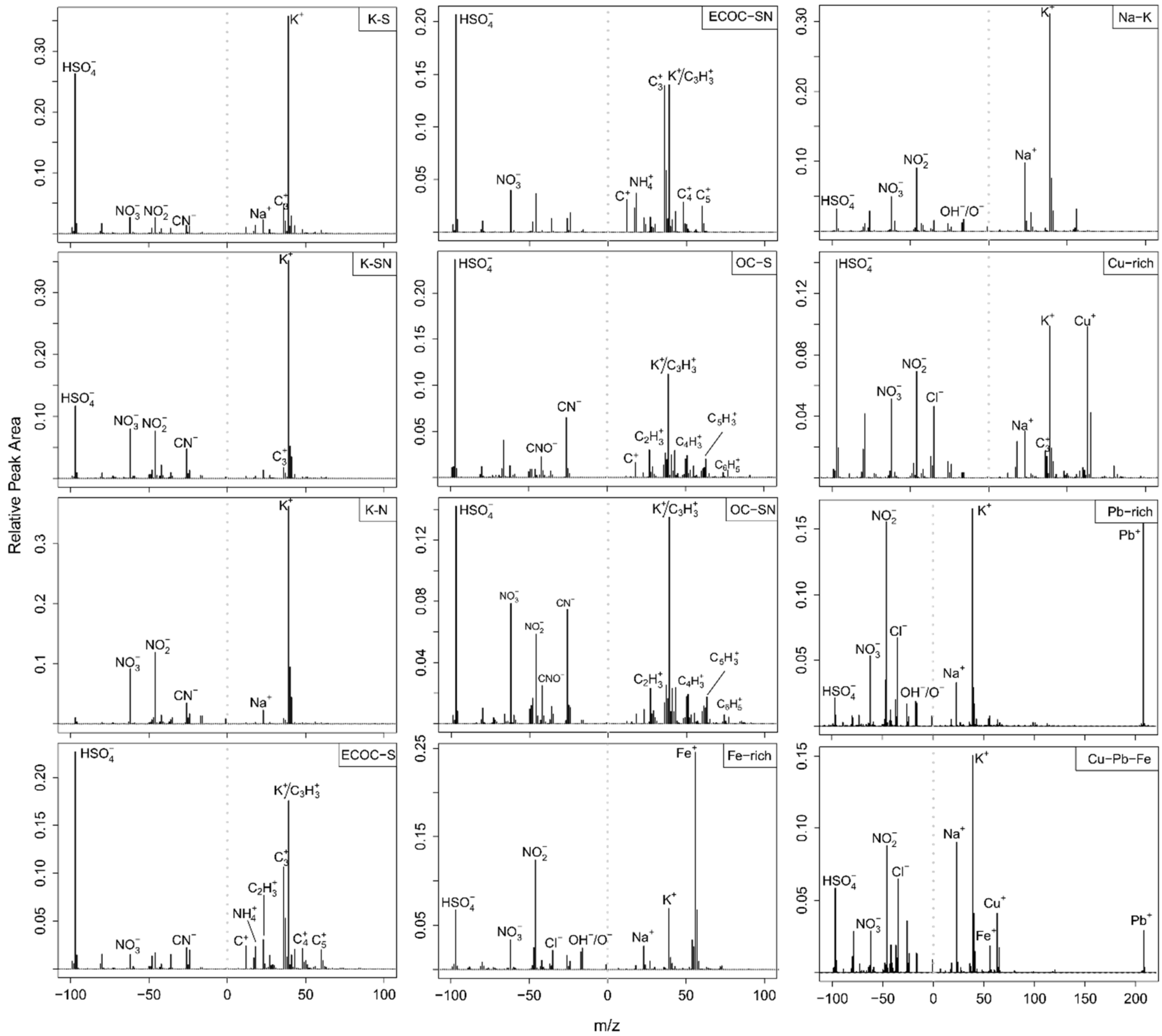

Fig. S3. Mass spectra for the observed single particle types in the atmosphere of Guangzhou during fall of 2012.

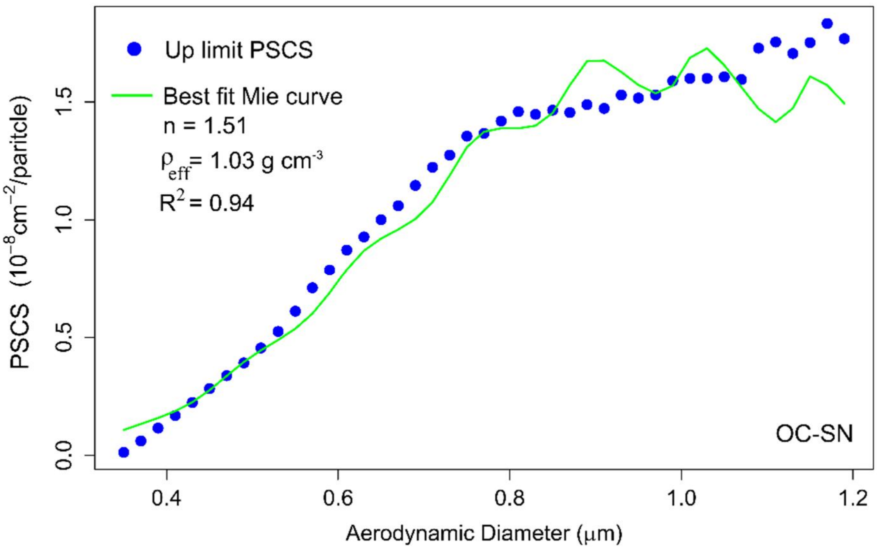

Fig. S4. Measured and best fit theoretical PSCS for OC-SN particle type.

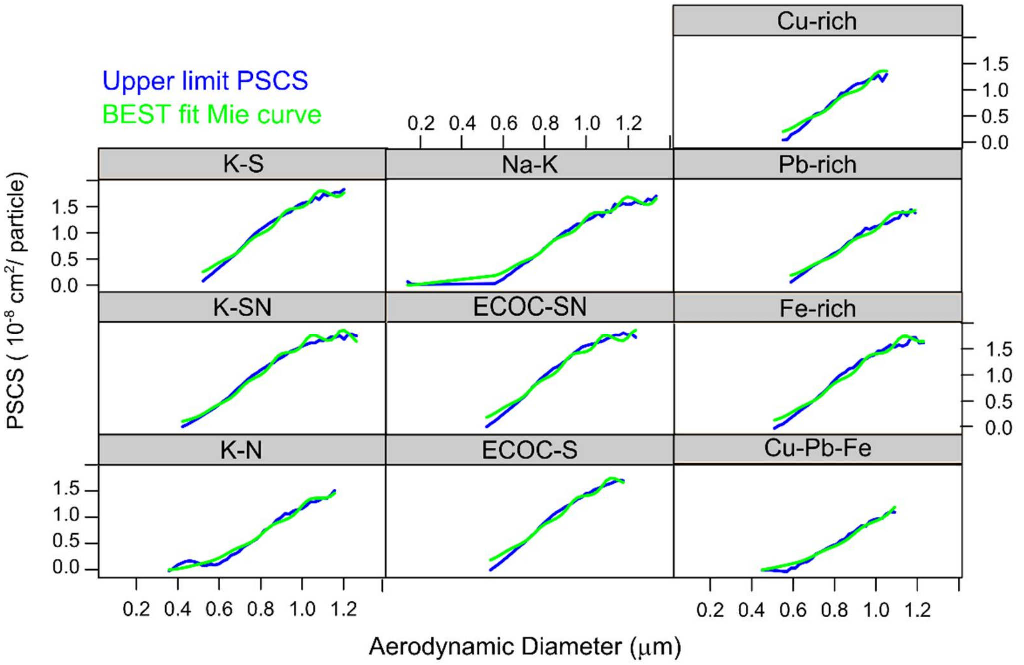

Fig. S5. Measured and best fit theoretical PSCS for various particle types observed in the present study.

REFERENCES

Gaston, C. J., H. Furutani, S. A. Guazzotti, K. R. Coffee, T. S. Bates, P. K. Quinn, L. I. Aluwihare, B. G. Mitchell, and K. A. Prather (2011), Unique ocean-derived particles serve as a proxy for changes in ocean chemistry, *J. Geophys. Res.-Atmos.*, *116*(D18310), 1-13, doi:10.1029/2010jd015289.

Gaston, C. J., P. K. Quinn, T. S. Bates, J. B. Gilman, D. M. Bon, W. C. Kuster, and K. A. Prather (2013), The impact of shipping, agricultural, and urban emissions on single particle chemistry observed aboard the R/V Atlantis during CalNex, *J. Geophys. Res.-Atmos.*, *118*(10), 5003-5017, doi:10.1002/Jgrd.50427.

Moffet, R. C., B. de Foy, L. T. Molina, M. J. Molina, and K. A. Prather (2008), Measurement of ambient aerosols in northern Mexico City by single particle mass spectrometry, *Atmos. Chem. Phys.*, *8*(16), 4499-4516.

Silva, P. J., D. Y. Liu, C. A. Noble, and K. A. Prather (1999), Size and chemical characterization of individual particles resulting from biomass burning of local Southern California species, *Environ. Sci. Technol.*, *33*(18), 3068-3076.

Silva, P. J., and K. A. Prather (2000), Interpretation of mass spectra from organic compounds in aerosol time-of-flight mass spectrometry, *Anal. Chem.*, *72*(15), 3553-3562.

Sodeman, D. A., S. M. Toner, and K. A. Prather (2005), Determination of single particle mass spectral signatures from light-duty vehicle emissions, *Environ. Sci. Technol.*, *39*(12), 4569-4580.

Song, X. H., P. K. Hopke, D. P. Fergenson, and K. A. Prather (1999), Classification of single particles analyzed by ATOFMS using an artificial neural network, ART-2A, *Anal. Chem.*, *71*(4), 860-865.

Zhang, G. H., B. X. Han, X. H. Bi, S. H. Dai, W. Huang, D. H. Chen, X. M. Wang, G. Y. Sheng, J. M. Fu, and Z. Zhou (2015), Characteristics of individual particles in the atmosphere of Guangzhou by single particle mass spectrometry, *Atmos. Res.*, *153*(0), 286-295, doi:10.1016/j.atmosres.2014.08.016.